Published in final edited form as:
Mol Cell. 2012 April 13; 46(1): 7–17. doi:10.1016/j.molcel.2012.01.019.

Histone H3 Lysine 56 Methylation Regulates DNA Replication through Its Interaction with PCNA

Yongxin Yu[1,3], **Chunying Song**[1,3], **Qiongyi Zhang**[1], **Peter A. DiMaggio**[2], **Benjamin A. Garcia**[2], **Autumn York**[1], **Michael F. Carey**[1], and **Michael Grunstein**[1,*]

[1]Molecular Biology Institute and Department of Biological Chemistry, David Geffen School of Medicine at UCLA, Los Angeles, CA, 90095, USA

[2]Department of Molecular Biology, Princeton University, Princeton, NJ, 08544, USA

SUMMARY

Histone modifications play important roles in regulating DNA-based biological processes. Of the modified sites, histone H3 lysine 56 (H3K56) is unique in that it lies within the globular core domain near the entry-exit sites of the nucleosomal DNA superhelix and its acetylation state in yeast is a marker for newly synthesized histones in transcription, DNA repair and DNA replication. We now report the presence of H3K56 monomethylation (H3K56me1) in mammalian cells and find that the histone lysine methytransferase G9a/KMT1C is required for H3K56me1 both in vivo and in vitro. We also find that disruption of G9a or H3K56 impairs DNA replication. Furthermore, H3K56me1 associates with the replication processivity factor PCNA primarily in G1 phase of the cell cycle and directly, in vitro. These results find H3K56me1 in mammals and indicate a role for H3K56me1 as a chromatin docking site for PCNA prior to its function in DNA replication.

INTRODUCTION

Histones carry diverse covalent modifications to regulate chromatin-dependent processes (Kouzarides, 2007). However, most research has been focused on residues within the unstructured N-terminal tails, which protrude from the nucleosome core to interact with various regulatory factors. In contrast, highly abundant (~30%) acetylation of K56 in the histone H3 globular domain has been identified in yeast and has been shown to mark histone assembly in various biological processes including transcription, DNA repair and replication (Han et al., 2007; Masumoto et al., 2005; Williams et al., 2008; Xu et al., 2005). H3K56 acetylation (H3K56ac) state has also been found to regulate yeast aging and the formation of heterochromatin (Feser et al., 2010; Xu et al., 2007). H3K56ac in mammals is much less abundant (~1%) and is associated with transcription of genes involved in pluripotency (Xie et al., 2009), chromatin assembly during DNA damage and repair (Das et al., 2009), genomic stability and DNA damage response (Tjeertes et al., 2009; Yuan et al., 2009). Interestingly, previous mass spectrometry studies also suggested the possibility of H3K56 methylation in mammalian cells (Garcia et al., 2007; Peters et al., 2003). However, H3K56 methylation has not been clearly identified and its biological significance remains unknown.

*Correspondence: Michael Grunstein, Tel: (310) 825-0840; Fax: (310) 206-9073; mg@mbi.ucla.edu.
[3]These authors contributed equally to the work

We show here that H3K56me1 exists in low abundance (~0.8%) in mammals where it serves as a docking site for PCNA in G1 of the cell cycle. Our data indicate that disrupting this interaction impairs subsequent DNA replication.

RESULTS

H3K56me1 Is Enriched at Chromatin Regions that Are Distinct from Those Involved in Transcription or Heterochromatin in Mammalian Cells

To address the presence and function of H3K56me1 we generated an antibody that recognizes H3K56me1 and validated its specificity by ELISA, competitive western blot and immunofluorescence, dot blot and western blot with histone modification analogs as shown in Figure S1. Using this antibody we show by western blot analysis that H3K56 is monomethylated in human cells (HeLa) but not in yeast (Figure 1A). To further confirm the presence of H3K56me1, we applied a sensitive mass spectrometry analysis by which a propionylated histone tryptic digest was analyzed (Plazas-Mayorca et al., 2009). A small fraction of H3 was identified as H3K56me1 in HeLa cells (~0.8% of total H3, Figure 1B) and in HEK293 cells (data not shown). We did not detect any di- or trimethylated H3K56 (Figure 1B). The presence of H3K56me1 was further verified by the tandem mass spectrum analysis (Figure 1C).

To demarcate the location of H3K56me1 in the nucleus, we compared its staining pattern to those of transcriptionally active and silent regions. We found that H3K56me1 is distributed throughout the nucleus in HeLa cells in a punctate staining pattern and shows no obvious colocalization with RNA Pol II (Figure 2A). Moreover, H3K56me1 is largely excluded from transcriptionally silent heterochromatin regions, which are DAPI-dense (Figure 2B) and which are enriched for Heterochromatin Protein 1α (HP1α) (Figure 2C). The exclusion of H3K56me1 from heterochromatin was also observed in mouse NIH3T3 fibroblast cells and human MCF7 breast epithelial cells (data not shown). Collectively, these results confirm that a small, but significant fraction of histone H3 is monomethylated at K56 in mammals and suggest that most H3K56me1 is involved in functions distinct from those in transcription and heterochromatin.

G9a Is Required for H3K56me1 in vivo and in vitro

In order to investigate H3K56me1 function in vivo we next wished to identify the histone methyltransferase (HMTase) required for H3K56me1 and screened a number of known HMTases by small interference RNA (siRNA) treatment in human HeLa cells. We found that siRNA knockdown of histone methyltransferases SET8, Ezh2, SETDB1/SETDB2 and Suv39h1/Suv39h2 decreased the level of these HMTases significantly in each case as assayed by western blots. However there was no obvious decrease in H3K56me1 level in any of these knockdown experiments (Figure 3A). In contrast, knockdown of G9a, the HMTase responsible for H3K9me1 and H3K9me2 in vivo (Peters et al., 2003; Rice et al., 2003; Tachibana et al., 2002), significantly decreased the H3K56me1 level (Figure 3B). Further, we found in G9a knockout mouse embryonic stem cells ($G9a^{-/-}$ ESCs) (Tachibana et al., 2002) that H3K56me1 is decreased as assayed by western blot (Figure 3C). The H3K56me1 signal is highly specific, as it was competed away by the H3K56me1 peptide but not H3K9me1 or H3K9me2 containing peptides (Figure S2A–S2B). Finally, using immunofluroscence we found that the staining of H3K56me1 is reduced strongly in $G9a^{-/-}$ ESCs (Figure 3D). Since G9a also methylates H3K9me1 and H3K9me2 we wished to distinguish the cellular sites at which K9 and K56 methylation occur. We found by immunofluorescence that there is no obvious colocalization between H3K56me1 and H3K9me1 or H3K9me2 in HeLa cells (Figure S2C–S2D). We conclude that there is little

overlap in cellular location of H3K56me1 and either H3K9me1 or H3K9me2 and that G9a is required for H3K56me1 in vivo.

To ask whether G9a possesses activity for H3K56me1 in vitro we used as our substrate recombinant H3 containing the tri-methyl lysine analog at K9 ($H3K_C9me3$), which cannot be methylated by G9a at H3K9 in vitro. We found that G9a mono-methylates histone H3 at lysine 56 in vitro as assayed by western blot analysis (Figure 3E). Given that G9a also methylates H3K27 in vitro (Tachibana et al., 2001), we wished to demonstrate that our antibody signal for H3K56me1 is not contaminated by possible recognition of H3K27me1. We find that the H3K56me1 signal is competed away completely by the peptide containing H3K56me1 but not by H3K27me1 peptide (Figure S2E). To confirm these findings we used recombinant H3 with a K9C substitution as the substrate for G9a HMTase activity and then analyzed the products by mass spectrometry. This experiment demonstrates that G9a directly monomethylates H3K56 at a low level (1.2%) similar to that of H3K56me1 in vivo (Figure S2F). Therefore, G9a is required for H3K56me1 in vivo and in vitro. While we cannot rule out the possibility that other HMTases also methylate H3K56 or that unknown cofactors are important for higher catalytic efficiency and specificity of G9a towards H3K56 at specific chromosomal loci, our data indicate that H3K56me1 level can be regulated in vivo by G9a.

Disruption of G9a or H3K56 Impairs DNA Replication

It is known that G9a is involved in early embryonic development and G9a deficient embryos display growth defects (Tachibana et al., 2002), however, the underlying mechanism remains unclear. To investigate the role of G9a in cell growth, we first examined cell cycle progression of $G9a^{-/-}$ ESCs. We found that passage through S phase was significantly delayed in $G9a^{-/-}$ ESCs after recovery from nocodazole-induced mitotic arrest. The results are shown in Figure 4A. Four hours after release, the DNA content of $G9a^{+/+}$ ESCs and $G9a^{-/-}$ ESCs indicated that the entry into S phase was similar. However, 10 hours after the release from nocodazole arrest ~ 86% of $G9a^{-/-}$ ESCs are still in S phase as compared to ~ 55% of $G9a^{+/+}$ ESCs. Since these findings suggest that DNA replication may be defective, we investigated DNA replication more directly by measuring incorporation of EdU (5-ethynyl-2′-deoxyuridine) in asynchronous $G9a^{-/-}$ ESCs via flow cytometry analysis. We found that loss of G9a led to a partial “collapse” of the arc of S phase cells and that the median intensity of incorporated EdU was significantly decreased in $G9a^{-/-}$ ESCs (Figure 4B). This suggests that $G9a^{-/-}$ ESCs incorporate less EdU in S phase and the improper S-phase progression of $G9a^{-/-}$ ESCs likely results from defective DNA replication. This delay in S phase is not due to a checkpoint response since Chk1, the key effector kinase activated by ATR in response to replicative-stress induced DNA damage (Smits et al., 2010), is not activated (phosphorylation at serine 345) and γH2AX level is not increased in $G9a^{-/-}$ ESCs (Figure 4C). We also used siRNA to knock down G9a in HeLa cells and found that depletion of G9a results in a significant S-phase accumulation of these cells that is not mediated by the DNA damage checkpoint response (data not shown). Therefore, our data indicate that DNA replication is impaired in G9a deficient cells.

It is known that G9a colocalizes with BrdU incorporation sites via its direct interaction with DNMT1 (Esteve et al., 2006). Since G9a knockdown may also affect DNA replication through such interactions we wished to ask whether mutating histone H3K56 or H3K9 specifically disrupts DNA replication. To do so we used HeLa cells expressing replication-dependent histone H3.1 bearing K56 or K9 substitutions (Tagami et al., 2004; Yuan et al., 2009). We found that compared to the wild type, a greater fraction of cells accumulates in S phase when expressing H3.1 K56 mutant constructs (K56A, K56R, K56Q) (Figure 4D). In contrast, the H3.1 K9A mutant did not significantly affect cell cycle progression. In addition, we found that the cells expressing replication-independent histone H3.3 bearing

K56Q and K56R mutants did not accumulate in S phase more than H3.3 WT cells (Figure 4D). Together, these data argue that H3K56me1 promotes passage through S phase and is important for efficient DNA replication.

The defect in DNA replication caused by lack of H3K56me1 led us to investigate whether the replication machinery is affected by H3.1 K56 substitutions. At the replication fork, replication protein A (RPA) stabilizes the unwound DNA duplex and RFC protein is recruited to load proliferating cell nuclear antigen (PCNA) which encircles DNA at the fork in S phase. In this manner, PCNA provides a platform on chromatin for the interaction of many replication factors (Branzei and Foiani; Moldovan et al., 2007; Sclafani and Holzen, 2007; Waga and Stillman, 1998). We found that histone H3.1 K56 substitution (K56A) has little if any effect on either chromatin-associated RPA or RFC however, chromatin-bound PCNA is significantly decreased in cells expressing H3.1 K56A (Figure 4E). We then compared the effect of replication-dependent H3.1 and replication-independent H3.3 mutations on PCNA levels. We found that the H3.1 K56 substitutions decreased chromatin-bound PCNA considerably, unlike H3.1 K9A or H3.3 K56 substitutions (Figure 4F). Therefore, these findings argue that H3.1 K56me1 facilitates efficient DNA replication by directly or indirectly affecting PCNA levels on chromatin.

H3K56me1 Directly Associates with PCNA

We next asked whether PCNA interacts with H3K56me1. As shown in Figure 5A, PCNA in nuclear extracts of HeLa cells or mouse Raw 264.7 cells is pulled down by the biotinylated H3 peptide bearing K56me1. In contrast, we were unable to detect a similar association of PCNA with H3 peptides trimethylated at K56 or monomethylated at K9 (Figure 5A). As a negative control, we show that the H3K56me1 peptide does not bind to the histone chaperone Asf1a/1b (Figure 5A) which interacts with H3/H4 (Groth et al., 2007). To address whether the interaction of PCNA with H3K56me1 is direct, we further performed the pull-down assay using purified recombinant PCNA and found that PCNA binds to the H3 peptide preferentially when K56 is monomethylated (Figure 5B). To ensure that the interaction between H3K56me1 and PCNA is not limited to short peptides, we assembled histone octamers with unmodified histone H3.1 or H3.1 K_C56me1 for the pull-down experiment with purified PCNA. Given that in our pull-down binding buffer conditions (0.5M NaCl), the octamers would dissociate to H3/H4 tetramers and H2A/H2B dimers (Eickbush and Moudrianakis, 1978), our data indicate that PCNA binds preferentially to H3/H4 tetramers containing K_C56me1 (Figure 5C). H3.1 K_C56me1 does not prevent nucleosome formation in vitro (data not shown). Nevertheless, we did not see binding of PCNA to H3.1 K_C56me1 assembled in a nucleosome (data not shown). Since DNA wrapped around the histone octamer may make K56 inaccessible (Luger et al., 1997), this argues that binding of PCNA to the nucleosome may require a cofactor or nucleosome remodeler. This is reminiscent of the function of CoREST in demethylation of nucleosomal H3K4me2 by LSD1 (Lee et al., 2005; Shi et al., 2005). In conclusion, a peptide containing H3K56me1 pulls down PCNA from nuclear extract. Moreover, recombinant PCNA binds directly to H3K56me1 peptide and also to H3K_C56me1-H4 tetramers in vitro. These data support a direct interaction between PCNA and histone H3.1 that is monomethylated at K56.

H3K56me1 Associates with PCNA in a Cell Cycle Specific Manner

Using co-immunoprecipitation we have shown that PCNA interacts in vivo with H3K56me1 but not with H3K9me1 (Figure S3A–S3B). While the H3K56me1 level is unchanged during the cell cycle in HeLa cells (data not shown), PCNA synthesis begins in G1 (Kurki et al., 1986) but encircles DNA and becomes detergent resistant only when cells enter S phase of the cell cycle (Waga and Stillman, 1998). In light of this, we wished to examine whether the

interaction between PCNA and H3K56me1 is regulated in a cell cycle specific manner. This was done using two independent approaches.

First, we applied an immunoprecipitation assay using HeLa cells released from double thymidine block (synchronized in S phase) or nocodazole block (synchronized in G1 phase). We found that PCNA co-immunoprecipitates with H3K56me1 with maximum association observed in G1 phase (Figure 5D). The association between H3K56me1 and PCNA is significantly decreased when cells enter S phase (Figure 5D). Second, we used the in situ proximity ligation assay (PLA), in which protein-protein interactions are visualized as fluorescent spots by rolling-circle amplification reactions dependent on the close proximity (< 40 nm) of the target proteins (Greenberg et al., 2008; Soderberg et al., 2006; Zhu et al., 2011). We found that the non-S phase population of asynchronous HeLa cells (EdU negative) preferentially shows greatly increased formation of PCNA-K56me1 complexes visualized as the red PLA spots (Figure 5E). Similar results were obtained in asynchronous NIH 3T3 cells (Figure S3C–S3D). However, neither H3K9me1 nor H3K9me2 associates with PCNA when assayed by PLA, suggesting that the H3K56me1 specifically binds to PCNA (Figure S3E–S3I). We then assayed PCNA-K56me1 complex formation during the cell cycle using synchronized HeLa cells. Our data demonstrate that PCNA-K56me1 complexes form preferentially in G1 (Figure 5F). Therefore, while PCNA has been assumed to be soluble or bound non-specifically to chromatin in G1, our data indicate that PCNA interacts in G1 with chromatin modified by H3K56me1. This may be interpreted to mean that H3K56me1 provides a chromatin docking site for PCNA in G1.

DISCUSSION

Our study establishes the presence of H3K56me1 in mammals, and demonstrates that the histone methyltransferase G9a is required for H3K56me1 in vivo and in vitro. We further show that G9a or H3K56 disruption, but not that of H3K9, results in decreased EdU incorporation indicating a defect in DNA replication that leads to the accumulation of cells in S phase. We find that H3K56me1 interacts in vivo and in vitro with PCNA, which provides a clue to the role of H3K56me1 in DNA replication. PCNA binding to chromatin requires replication-dependent H3.1 K56 but not H3.1 K9. Finally, our data indicate that PCNA interacts with H3K56me1 preferentially in G1 phase of the cell cycle. Since disruption of this interaction leads to defective PCNA recruitment to chromatin and DNA replication in S phase we propose that PCNA docking in G1 at H3K56me1 in chromatin facilitates the subsequent function of PCNA as a processivity factor in S phase. This is reminiscent of many cell division cycle mutants in yeast, in which the primary defect precedes the diagnostic landmark (Hartwell, 1978; Pringle, 1978).

G9a/KMT1C was initially described as a methyltransferase responsible for H3K9me1 and H3K9me2 (Tachibana et al., 2002). More recently, G9a has also been shown to methylate histone H1 (Trojer et al., 2009; Weiss et al., 2010) and non-histone substrates (Huang and Berger, 2008; Rathert et al., 2008). We report here that G9a disruption results in significantly decreased histone H3K56me1 in vivo. However, we find there is some residual H3K56me1 in $G9a^{-/-}$ ESCs. This is not due to the presence of G9a like protein GLP/KMT1D as we have knocked down GLP in $G9a^{-/-}$ cells and found that the residual H3K56me1 is unchanged (data not shown). This is expected from the cooperative activities of G9a and GLP that are present in the same enzymatic complex (Tachibana et al., 2005). Therefore G9a may not be the only HMTase responsible for H3K56me1 in vivo. We also find that G9a generates H3K56me1 at a low level (~1.2%) in vitro. Interestingly, K9 and K56 lie within a K-S-T motif (RK_9ST; $QK_{56}ST$), which may help explain why G9a can target these two lysines. While the R residue (RK_9ST) has been shown to be required for methylating G9a targets in vitro (Rathert et al., 2008) this requirement is not absolute as

histone H1.2 is methylated in vivo and in vitro by G9a/Glp1 at a C-terminal target site lacking this arginine (Weiss et al., 2010). The mechanism whereby G9a selects specific sites and whether the limited sequence similarity around K9 and K56 (RK_9ST; $QK_{56}ST$) (or additional cofactors) play a role in substrate selection in vivo (Rathert et al., 2008) remain topics for further study.

In this study we provide evidence suggesting a specific role for H3K56me1 in the regulation of DNA replication. In yeast, H3K56ac plays a role in replication-coupled nucleosome assembly (Li et al., 2008), and in mammals H3K56ac is required for proper nucleosome assembly during DNA damage response (Das et al., 2009; Yuan et al., 2009). Theoretically, we cannot exclude the possibility that lack of H3K56ac may cause a DNA replication defect. However, if it does so H3K56ac functions through a mechanism distinct from H3K56me1, since H3K56ac does not associate with PCNA when assayed by PLA (Figure S4). Moreover, H3K56ac increases upon genotoxic stress and localizes to the DNA damage foci (Das et al., 2009; Yuan et al., 2009,), probably due to its role in chromatin assembly (Das et al., 2009). However, unlike H3K56ac, H3K56me1 remains unchanged and does not localize to DNA damage loci upon gamma irradiation (Figure S5). This indicates that H3K56 acetylation and monomethylation have distinct cellular functions.

While PCNA synthesis begins in G1 (Kurki et al., 1986), it encircles DNA and becomes detergent resistant, which has been operationally defined as chromatin-bound, only when cells enter S phase of the cell cycle (Mukherjee et al., 2009; Waga and Stillman, 1998). However, the majority of PCNA has been assumed to be soluble or bound non-specifically, especially in G1 where it can be washed away by detergent most likely since it does not encircle DNA. Our data indicate that PCNA binds to H3K56me1 in G1 and that its disruption impairs PCNA recruitment to chromatin and DNA replication in S phase. At this stage, we can only speculate as to the function of H3K56me1 in this interaction. Providing an H3K56me1 docking site in G1 may increase the effective concentration for PCNA in subsequent replication. Alternatively, since PCNA serves as a platform in S phase for a large number of factors involved in replication, the binding of PCNA to H3K56me1 may prevent the recruitment of factors to PCNA in G1 that must only be recruited in S phase. The detailed mechanism by which H3K56me1 regulates PCNA function in DNA replication remains an interesting topic for future study.

EXPERIMENTAL PROCEDURES

Cell Culture

HeLa cells, MCF7 cells, NIH 3T3 cells and HEK293 cells were grown in DMEM media supplemented with 10% FBS. ES cells were maintained in DMEM containing leukemia inhibitory factor (LIF), Non Essential Amino Acids, 2-mercaptoethanol and 10% defined FBS.

Mass Spectrometry

Histones purified from HeLa and HEK293 cells were prepared essentially as previously published using the “one-pot” proteomics procedure (Plazas-Mayorca et al., 2009). Trypsin digested propionylated histones were desalted using homemade StageTips as previously described (Plazas-Mayorca et al., 2009), and the samples were analyzed by nanoflowLC-MS on an Orbitrap mass spectrometer operated as previously described (Plazas-Mayorca et al., 2009). All data were manually inspected. A detailed description can also be found in the Supplemental Experimental Procedures.

In vitro HMTase Assay

The methyltransferase assay was performed as described previously with modifications (Tachibana et al., 2001). Briefly, 1μg of recombinant histone H3 that has tri-methyl lysine analog at K9 (Active Motif) or bears a K9C mutation and 0.25 μg, 0.5 μg or 1 μg of recombinant G9a (Active Motif) was added to the methyltransferase activity buffer (80 μM *S*-adenosylmethionine, 50 mM Tris, pH 9.0, 0.5 mM dithiothreitol) to yield 25 μl final volume and incubated at 37°C for 60 min. The reaction products were analyzed by western blot or mass spectrometry analysis.

Pull-down Assays

Biotinylated H3 peptides unmodified, mono- or trimethylated at K56 or K9 were prebound to avidin agarose beads, incubated with nuclear extracts or purified recombinant PCNA at 4°C and the bound proteins were analyzed by SDS-PAGE and western blot. A detailed description can also be found in the Supplemental Experimental Procedures.

FACS Analysis

To measure the cell cycle profile, cells were trypsinized, washed and fixed in ice-cold ethanol at 4°C for at least 12 hrs. Immediately before flow cytometric analysis, the cells were permeabilized and stained with propidium iodide for 20 minutes, then subjected to FACS analysis using FACSCalibur Analytic Flow cytometer. A detailed description can also be found in the Supplemental Experimental Procedures.

in situ Proximity Ligation Assay (PLA)

In situ PLA in combination with immunofluorescence confocal microscopy was performed to detect physically protein–protein interactions using Duolink II Detection Kit with PLA PLUS and MINUS Probes for mouse and rabbit according to the manufacturer's protocol (Olink Bioscience). A detailed description can also be found in the Supplemental Experimental Procedures.

Statistical Analysis

Statistical significance evaluation was assessed using Student's *t*-test, with a two-tailed distribution and assuming unequal sample variance. Data are presented as the mean ± standard error of the mean (s.e.m.). The number of repeated experiments and the number of cells used for PLA signal counting or for Pearson's correlation coefficients calculation (*n*) are indicated in the legends.

Supplementary Material

Refer to Web version on PubMed Central for supplementary material.

Acknowledgments

We are grateful to Wei Xie, Adam Sperling and members of the Grunstein laboratory for generous help and critical discussion throughout this work. In addition, we thank Lin Jiang and Dr. David Eisenberg for helpful advice, Dr. Yoichi Shinkai for providing G9a wild-type and knockout ES cells, Dr. Bruce Stillman for providing ORC2 antibodies (pAb205, mAb920), Dr. Kathrin Plath for providing the FLAG-tagged H3.1 and H3.3 plasmids, Dr. Arnold Berk and Carol Eng for assistance with cell culture, Lynn Lehmann for providing $H3K_C9$ histones. Y.Y. is especially grateful to Bing Li for critical advice throughout this work. This work was supported by the National Institutes of Health grant GM-23674 to M.G.

References

Branzei D, Foiani M. Maintaining genome stability at the replication fork. Nat Rev Mol Cell Biol. 11:208–219. [PubMed: 20177396]

Das C, Lucia MS, Hansen KC, Tyler JK. CBP/p300-mediated acetylation of histone H3 on lysine 56. Nature. 2009; 459:113–117. [PubMed: 19270680]

Eickbush TH, Moudrianakis EN. The histone core complex: an octamer assembled by two sets of protein-protein interactions. Biochemistry. 1978; 17:4955–4964. [PubMed: 718868]

Esteve PO, Chin HG, Smallwood A, Feehery GR, Gangisetty O, Karpf AR, Carey MF, Pradhan S. Direct interaction between DNMT1 and G9a coordinates DNA and histone methylation during replication. Genes Dev. 2006; 20:3089–3103. [PubMed: 17085482]

Feser J, Truong D, Das C, Carson JJ, Kieft J, Harkness T, Tyler JK. Elevated histone expression promotes life span extension. Mol Cell. 2010; 39:724–735. [PubMed: 20832724]

Garcia BA, Hake SB, Diaz RL, Kauer M, Morris SA, Recht J, Shabanowitz J, Mishra N, Strahl BD, Allis CD, et al. Organismal differences in post-translational modifications in histones H3 and H4. J Biol Chem. 2007; 282:7641–7655. [PubMed: 17194708]

Greenberg JI, Shields DJ, Barillas SG, Acevedo LM, Murphy E, Huang J, Scheppke L, Stockmann C, Johnson RS, Angle N, et al. A role for VEGF as a negative regulator of pericyte function and vessel maturation. Nature. 2008; 456:809–813. [PubMed: 18997771]

Groth A, Corpet A, Cook AJ, Roche D, Bartek J, Lukas J, Almouzni G. Regulation of replication fork progression through histone supply and demand. Science. 2007; 318:1928–1931. [PubMed: 18096807]

Han J, Zhou H, Horazdovsky B, Zhang K, Xu RM, Zhang Z. Rtt109 acetylates histone H3 lysine 56 and functions in DNA replication. Science. 2007; 315:653–655. [PubMed: 17272723]

Hartwell LH. Cell division from a genetic perspective. J Cell Biol. 1978; 77:627–637. [PubMed: 355261]

Huang J, Berger SL. The emerging field of dynamic lysine methylation of non-histone proteins. Curr Opin Genet Dev. 2008; 18:152–158. [PubMed: 18339539]

Kouzarides T. Chromatin modifications and their function. Cell. 2007; 128:693–705. [PubMed: 17320507]

Kurki P, Vanderlaan M, Dolbeare F, Gray J, Tan EM. Expression of proliferating cell nuclear antigen (PCNA)/cyclin during the cell cycle. Exp Cell Res. 1986; 166:209–219. [PubMed: 2874992]

Lee MG, Wynder C, Cooch N, Shiekhattar R. An essential role for CoREST in nucleosomal histone 3 lysine 4 demethylation. Nature. 2005; 437:432–435. [PubMed: 16079794]

Li Q, Zhou H, Wurtele H, Davies B, Horazdovsky B, Verreault A, Zhang Z. Acetylation of histone H3 lysine 56 regulates replication-coupled nucleosome assembly. Cell. 2008; 134:244–255. [PubMed: 18662540]

Luger K, Mader AW, Richmond RK, Sargent DF, Richmond TJ. Crystal structure of the nucleosome core particle at 2.8 A resolution. Nature. 1997; 389:251–260. [PubMed: 9305837]

Masumoto H, Hawke D, Kobayashi R, Verreault A. A role for cell-cycle-regulated histone H3 lysine 56 acetylation in the DNA damage response. Nature. 2005; 436:294–298. [PubMed: 16015338]

Moldovan GL, Pfander B, Jentsch S. PCNA, the maestro of the replication fork. Cell. 2007; 129:665–679. [PubMed: 17512402]

Mukherjee P, Cao TV, Winter SL, Alexandrow MG. Mammalian MCM loading in late-G(1) coincides with Rb hyperphosphorylation and the transition to post-transcriptional control of progression into S-phase. PLoS One. 2009; 4:e5462. [PubMed: 19421323]

Peters AH, Kubicek S, Mechtler K, O'Sullivan RJ, Derijck AA, Perez-Burgos L, Kohlmaier A, Opravil S, Tachibana M, Shinkai Y, et al. Partitioning and plasticity of repressive histone methylation states in mammalian chromatin. Mol Cell. 2003; 12:1577–1589. [PubMed: 14690609]

Plazas-Mayorca MD, Zee BM, Young NL, Fingerman IM, LeRoy G, Briggs SD, Garcia BA. One-pot shotgun quantitative mass spectrometry characterization of histones. J Proteome Res. 2009; 8:5367–5374. [PubMed: 19764812]

Pringle JR. The use of conditional lethal cell cycle mutants for temporal and functional sequence mapping of cell cycle events. J Cell Physiol. 1978; 95:393–405. [PubMed: 348711]

Rathert P, Dhayalan A, Murakami M, Zhang X, Tamas R, Jurkowska R, Komatsu Y, Shinkai Y, Cheng X, Jeltsch A. Protein lysine methyltransferase G9a acts on non-histone targets. Nat Chem Biol. 2008; 4:344–346. [PubMed: 18438403]

Rice JC, Briggs SD, Ueberheide B, Barber CM, Shabanowitz J, Hunt DF, Shinkai Y, Allis CD. Histone methyltransferases direct different degrees of methylation to define distinct chromatin domains. Mol Cell. 2003; 12:1591–1598. [PubMed: 14690610]

Sclafani RA, Holzen TM. Cell cycle regulation of DNA replication. Annu Rev Genet. 2007; 41:237–280. [PubMed: 17630848]

Shi YJ, Matson C, Lan F, Iwase S, Baba T, Shi Y. Regulation of LSD1 histone demethylase activity by its associated factors. Mol Cell. 2005; 19:857–864. [PubMed: 16140033]

Smits VA, Warmerdam DO, Martin Y, Freire R. Mechanisms of ATR-mediated checkpoint signalling. Front Biosci. 2010; 15:840–853. [PubMed: 20515729]

Soderberg O, Gullberg M, Jarvius M, Ridderstrale K, Leuchowius KJ, Jarvius J, Wester K, Hydbring P, Bahram F, Larsson LG, et al. Direct observation of individual endogenous protein complexes in situ by proximity ligation. Nat Methods. 2006; 3:995–1000. [PubMed: 17072308]

Tachibana M, Sugimoto K, Fukushima T, Shinkai Y. Set domain-containing protein, G9a, is a novel lysine-preferring mammalian histone methyltransferase with hyperactivity and specific selectivity to lysines 9 and 27 of histone H3. J Biol Chem. 2001; 276:25309–25317. [PubMed: 11316813]

Tachibana M, Sugimoto K, Nozaki M, Ueda J, Ohta T, Ohki M, Fukuda M, Takeda N, Niida H, Kato H, et al. G9a histone methyltransferase plays a dominant role in euchromatic histone H3 lysine 9 methylation and is essential for early embryogenesis. Genes Dev. 2002; 16:1779–1791. [PubMed: 12130538]

Tachibana M, Ueda J, Fukuda M, Takeda N, Ohta T, Iwanari H, Sakihama T, Kodama T, Hamakubo T, Shinkai Y. Histone methyltransferases G9a and GLP form heteromeric complexes and are both crucial for methylation of euchromatin at H3-K9. Genes Dev. 2005; 19:815–826. [PubMed: 15774718]

Tagami H, Ray-Gallet D, Almouzni G, Nakatani Y. Histone H3.1 and H3.3 complexes mediate nucleosome assembly pathways dependent or independent of DNA synthesis. Cell. 2004; 116:51–61. [PubMed: 14718166]

Tjeertes JV, Miller KM, Jackson SP. Screen for DNA-damage-responsive histone modifications identifies H3K9Ac and H3K56Ac in human cells. EMBO J. 2009; 28:1878–1889. [PubMed: 19407812]

Trojer P, Zhang J, Yonezawa M, Schmidt A, Zheng H, Jenuwein T, Reinberg D. Dynamic Histone H1 Isotype 4 Methylation and Demethylation by Histone Lysine Methyltransferase G9a/KMT1C and the Jumonji Domain-containing JMJD2/KDM4 Proteins. J Biol Chem. 2009; 284:8395–8405. [PubMed: 19144645]

Waga S, Stillman B. The DNA replication fork in eukaryotic cells. Annu Rev Biochem. 1998; 67:721–751. [PubMed: 9759502]

Weiss T, Hergeth S, Zeissler U, Izzo A, Tropberger P, Zee BM, Dundr M, Garcia BA, Daujat S, Schneider R. Histone H1 variant-specific lysine methylation by G9a/KMT1C and Glp1/KMT1D. Epigenetics Chromatin. 2010; 3:7. [PubMed: 20334638]

Williams SK, Truong D, Tyler JK. Acetylation in the globular core of histone H3 on lysine-56 promotes chromatin disassembly during transcriptional activation. Proc Natl Acad Sci U S A. 2008; 105:9000–9005. [PubMed: 18577595]

Xie W, Song C, Young NL, Sperling AS, Xu F, Sridharan R, Conway AE, Garcia BA, Plath K, Clark AT, et al. Histone h3 lysine 56 acetylation is linked to the core transcriptional network in human embryonic stem cells. Mol Cell. 2009; 33:417–427. [PubMed: 19250903]

Xu F, Zhang K, Grunstein M. Acetylation in histone H3 globular domain regulates gene expression in yeast. Cell. 2005; 121:375–385. [PubMed: 15882620]

Xu F, Zhang Q, Zhang K, Xie W, Grunstein M. Sir2 deacetylates histone H3 lysine 56 to regulate telomeric heterochromatin structure in yeast. Mol Cell. 2007; 27:890–900. [PubMed: 17889663]

Yuan J, Pu M, Zhang Z, Lou Z. Histone H3-K56 acetylation is important for genomic stability in mammals. Cell Cycle. 2009; 8:1747–1753. [PubMed: 19411844]

Zhu P, Tan MJ, Huang RL, Tan CK, Chong HC, Pal M, Lam CR, Boukamp P, Pan JY, Tan SH, et al. Angiopoietin-like 4 protein elevates the prosurvival intracellular O2(−):H2O2 ratio and confers anoikis resistance to tumors. Cancer Cell. 2011; 19:401–415.h. [PubMed: 21397862]

Highlights

- H3K56me1 is detected in mammals
- G9a/KMT1C is required for H3K56me1 in vivo and in vitro
- H3K56me1 facilitates DNA replication
- Replication factor PCNA binds preferentially to H3K56me1 in G1 phase

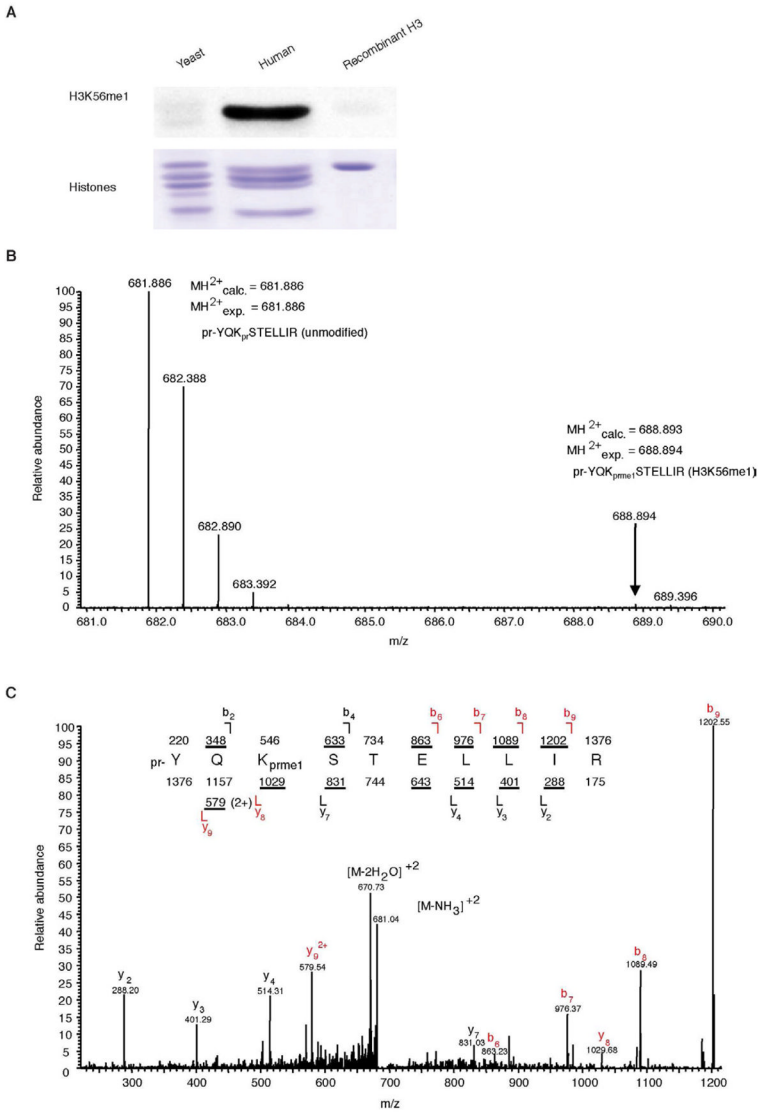

Figure 1. Histone H3K56 Is Monomethylated in Mammals

(A) Recombinant human histone H3 and purified histones from *S. cerevisiae* (yeast) and HeLa cells (human) were probed with α-H3K56me1 antibody. Equivalent amounts of proteins were loaded as shown by Coomassie blue staining. **(B)** Histones were isolated from HeLa cells and analyzed by mass spectrometry. Full mass spectrum is shown for unmodified (pr-YQK$_{pr}$STELLIR, 681 m/z) and monomethylated (pr-YQK$_{prme1}$STELLIR, 688 m/z) peptides from HPLC separated elutions. Accurate mass on the peptide at 688.894 m/z clearly indicates that the modification is a monomethylation mark. **(C)** Tandem mass spectrum of the monomethylated peptide (pr-YQK$_{prme1}$STELLIR) shows that the monomethylation modification is localized to the K56 residue. See also Figure S1.

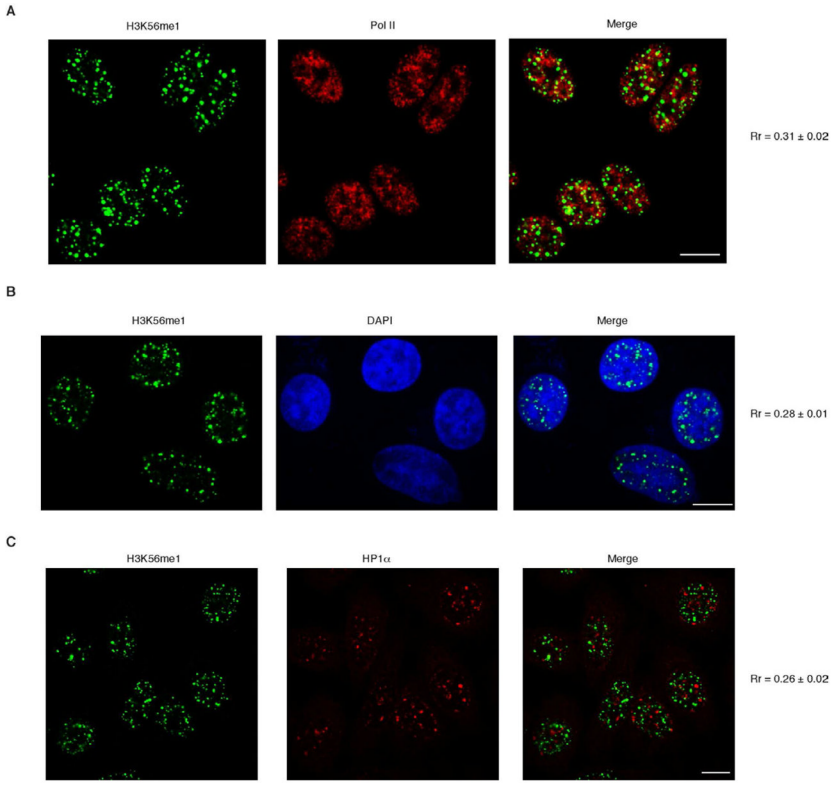

Figure 2. Subnuclear Localization of Histone H3K56me1

(A) Dual immunofluorescence staining of HeLa cells was performed using α-H3K56me1 and α-Pol II antibodies. H3K56me1 shows no obvious colocalization with Pol II. **(B)** Immunofluorescence staining showing that in HeLa cells H3K56me1 is distributed extensively throughout the nucleus, but is excluded from DAPI dense regions. **(C)** Dual immunofluorescence staining of HeLa cells was performed using α-H3K56me1 and α-HP1α antibodies. H3K56me1 shows no obvious colocalization with α-HP1α. Pearson's correlation coefficients (*Rr*) are calculated using ImageJ software. Data represent mean ± s.e.m., (**A,** n = 105; **B,** n = 89; **C,** n = 72). Cells were fixed with methanol without Triton X-100 pre-extraction. Scale bar, 10 μm.

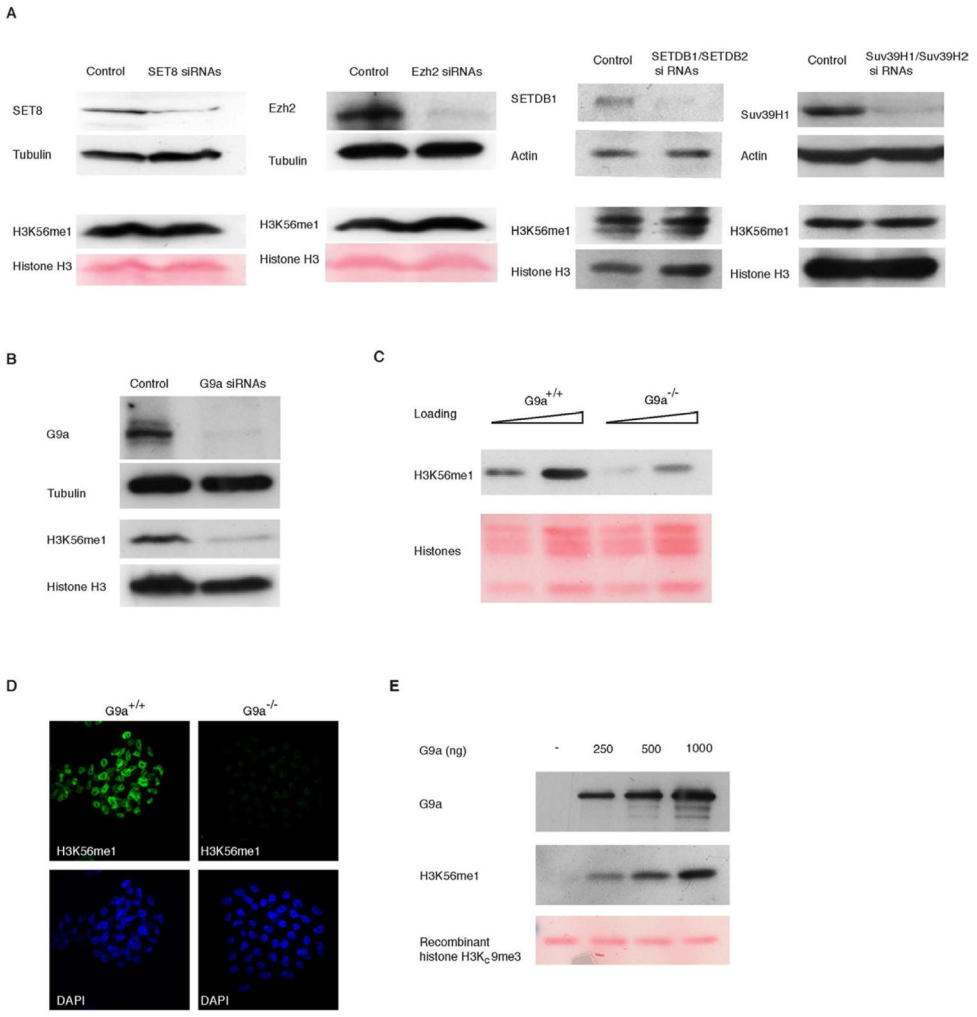

Figure 3. G9a Is Required for Histone H3K56 Monomethylation in vivo and in vitro

(A) HeLa cells were transfected with SET8, Ezh2, SETDB1/SETDB2, Suv39H1/Suv39H2 siRNAs or non-targeting siRNA (Control). Immunoblots showing that the expression of endogenous methyltransferases is decreased, while H3K56me1 level remains unchanged. **(B)** HeLa cells were transfected with non-targeting siRNA (Control) or G9a siRNAs. Immunoblot showing that the expression of endogenous G9a is decreased. Tubulin served as an internal control for protein loading. H3K56me1 is decreased in HeLa cells transfected with G9a siRNA compared to control, while endogenous histone H3 expression remains unchanged. **(C)** Nuclear extracts prepared from $G9a^{+/+}$ and $G9a^{-/-}$ ES cells were blotted with α-H3K56me1 antibody. $G9a^{-/-}$ ES cells showed a significant reduction of H3K56me1. Ponceau S staining of histones served as a loading control. **(D)** $G9a^{+/+}$ and $G9a^{-/-}$ ES cells were pre-extracted with 0.5% Triton X-100 and fixed with methanol. Immunofluorescence staining was performed using H3K56me1 antibody. $G9a^{+/+}$ ES cells showed extensive H3K56me1 staining while the $G9a^{-/-}$ ES cells exhibited a dramatic loss of H3K56me1 signal. Original magnification, ×64. **(E)** G9a HMTase activity for H3K56 was measured by in vitro HMTase assay using recombinant G9a. Substrate is recombinant H3 with tri-methyl lysine analog at K9 ($H3K_C9me3$). Immunoblot showing that H3 becomes monomethylated at K56 when incubated with G9a. Ponceau S staining indicates that equal amounts of histone H3 were used in each reaction. See also Figure S2.

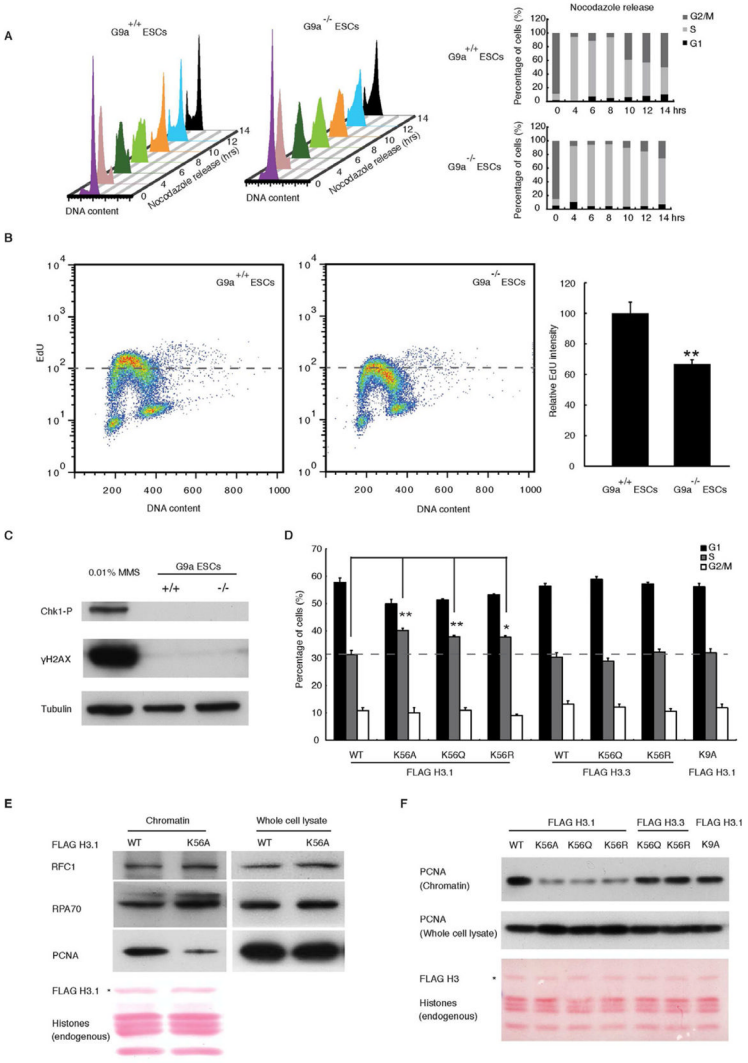

Figure 4. H3K56 Monomethylation Contributes to DNA Replication

(A) Loss of G9a leads to delayed passage through S phase. G9a$^{+/+}$ and G9a$^{-/-}$ ES cells were arrested in M phase by nocodazole treatment for 16 hrs, then released into the cell cycle. Cells were collected at indicated time points, fixed, stained with propidium iodide (PI), and DNA content was analyzed by FACS. Histograms of DNA content are shown (Left panels). The percentage of cells in G_1, S, and G_2/M phases of the cell cycle at each time point is shown (Right panel). **(B)** Inefficient DNA replication in G9a$^{-/-}$ ES cells was detected by EdU incorporation. Cells were pulse labeled with EdU for 5 min, fixed, stained for EdU and PI, and analyzed by FACS. Left panels: Plots of EdU incorporation against DNA staining with PI are shown. Note that there is a partial "collapse" of the arc of S phase population of G9a$^{-/-}$ ES cells. Right panels: Quantitation analysis showed that the median intensity of the incorporated EdU was decreased in G9a$^{-/-}$ ES cells compared to G9a$^{+/+}$ ES cells. Data are presented as mean±SEM from 6 experiments, **, $P < 0.01$. **(C)** Immunoblots show that the phosphorylation of Chk1, H2AX is not activated in G9a$^{-/-}$ ES cells. HEK293 cells treated with 0.01% MMS served as a positive control for checkpoint activation. **(D)** Lack of H3K56me1 leads to S-phase accumulation. HeLa cells were transfected with FLAG-tagged histone H3.1 or H3.3 wild type (WT) or K56 mutants (K56A, K56R, K56Q) or H3.1 K9A.

The cells were fixed, incubated with anti-FLAG antibody, followed by secondary antibody conjugated to Alexa Fluor 647. The DNA content against PI staining of FLAG-tagged positive cells was analyzed by FACS and the percentage of cells in each stage of the cell cycle showing an accumulation in S phase when expressing H3.1K56 mutants. Data are presented as mean±SEM from at least 3 experiments, *, $P < 0.05$, **, $P < 0.01$. **(E)** Lack of H3K56me1 impairs PCNA binding to chromatin. The chromatin fraction was extracted from HeLa cells transfected with FLAG-tagged H3.1 WT or H3.1 K56A mutant and the levels of PCNA, RPA70 and RFC1 were measured by western blot. Immunoblot showing that the chromatin-bound PCNA is decreased in cells expressing H3.1K56A mutant. Neither chromatin-associated RPA70 nor RFC1 was decreased (left upper panels). Ponceau S staining showing that both wild type H3.1 and H3.1K56A incorporated into chromatin equally (left bottom panel). The levels of PCNA, RFC1, RPA70 in the whole cell lysate were unchanged (right panels). **(F)** Immunoblots showing that chromatin-bound PCNA is decreased in HeLa cells expressing H3.1K56 mutants but not H3.1K9A or H3.3K56 mutants. The level of PCNA in the whole cell lysate was unchanged (middle panel). Ponceau S staining showing that both wild type H3 and mutant H3 incorporated into chromatin equally (bottom panel).

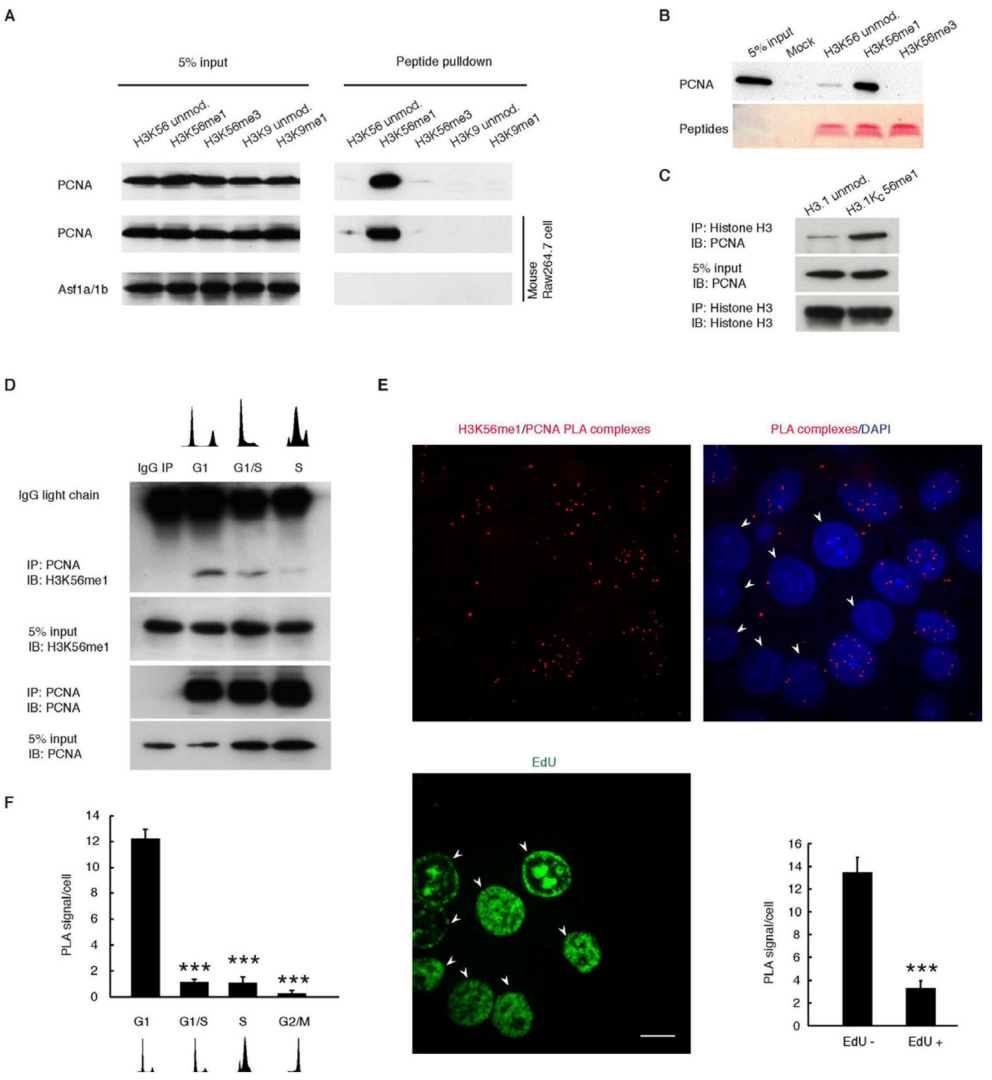

Figure 5. Histone H3K56 Monomethylation Associates with PCNA Specifically in A Cell Cycle Dependent Manner

(A) Nuclear extracts from human (HeLa cells) or mouse (Raw264.7 cells) were used in peptide pull-down assays with a series of biotinylated H3 peptides, either unmodified (unmod.) or methylated as indicated. PCNA was pulled down specifically by the H3K56me1 peptide (top and middle panels). None of the peptides associated with Asf1a/1b (bottom panels). **(B)** Peptide pull-down assay with purified recombinant PCNA and H3 peptides either unmodified or methylated as indicated. Recombinant PCNA was pulled down specifically by the H3K56me1 peptide. **(C)** Histone octamers with unmodified histone H3.1 (H3.1 unmod.) or H3.1 K_C56me1 were assembled for the pull-down experiment with purified PCNA. It should be noted that the octamers would dissociate to H3/H4 tetramers and H2A/H2B dimers under our binding buffer conditions (0.5M NaCl) (Eickbush and Moudrianakis, 1978). PCNA was associated with the H3.1 K_C56me1-H4 tetramer (top panel). Histone H3.1-H4 tetramer was equally immunoprecipitated by histone H3 antibody (bottom panel) and equal amounts of PCNA were used in the experiment (middle panel). **(D)** Nuclear fractions were prepared from synchronized HeLa cells and immunoprecipitated with α-PCNA antibody. Immunoblot showing that PCNA associated with H3K56me1 in G1, whereas the association decreased dramatically during S phase. Flow cytometry profiles are

shown above the panels. **(E)** HeLa cells were incubated with EdU for 30 min, fixed with methanol without Triton X-100 pre-extraction and immunofluorescence confocal microscopy in combination with in situ PLA was performed. The incorporated EdU was stained using Click-iT® EdU Alexa Fluor® 488 Imaging Kit. Nuclei were stained with DAPI. Red dots in the confocal microscopic images indicate physically interacting H3K56me1/PCNA complexes. Note that H3K56me1/PCNA complex predominantly occurs in non-S phase cells. S phase cells incorporate EdU as indicated by arrowheads. Scale bar, 10 μm. Lower right panel: Quantification of the PLA signal in HeLa cells in two independent experiments (EdU-, n = 58; EdU+, n = 32; Mean ± s.e.m., ***, $P < 0.001$). **(F)** Quantification of the mean number of PLA signals in synchronized HeLa cells in at least two independent experiments (G1, n = 93; G1/S, n = 150; S, n = 193; G2/M, n = 79; Mean ± s.e.m., ***, $P < 0.001$). Flow cytometry profiles are shown below the bar graph panel. See also Figure S3.